Role of the Intercrystalline Tie Chains Network in the Mechanical Response of Semicrystalline Polymers

Sara Jabbari-Farouji*
Institute of Physics, Johannes Gutenberg-University, Staudingerweg 7-9, 55128 Mainz, Germany

Olivier Lame and Michel Perez
Université de Lyon, INSA, MATEIS, UMR CNRS 5510, F69621 Villeurbanne, France

Joerg Rottler
Department of Physics and Astronomy, University of British Columbia, 6224 Agricultural Road, Vancouver, British Columbia V6T 1Z1, Canada

Jean-Louis Barrat
Université Grenoble Alpes, LIPHY, F-38000 Grenoble, France and CNRS, LIPHY, F-38000 Grenoble, France
(Received 13 September 2016; revised manuscript received 26 March 2017; published 26 May 2017)

We examine the microscopic origin of the tensile response in semicrystalline polymers by performing large-scale molecular dynamics simulations of various chain lengths. We investigate the microscopic rearrangements of the polymers during tensile deformation and show that the intercrystalline chain connections known as tie chains contribute significantly to the elastic and plastic response. These results suggest that the mechanical behavior of semicrystalline polymers is controlled by two interpenetrated networks of entanglements and tie chains.

DOI: 10.1103/PhysRevLett.118.217802

Mechanical properties of polymeric materials strongly depend on their morphology [1]. Semicrystalline polymers, composed of ordered and amorphous regions, are of great technological interest as they combine the strength of purely crystalline materials with the strain hardening of fully amorphous polymers. Establishing a link between the underlying structure and mechanical properties is one of the major challenges in polymer physics and has been the subject of intense research [2]. It still remains unclear how the interplay of the entangled amorphous network with the crystalline domains determines their mechanical response.

Experiments suggest that the molecular connections between the crystallites, so-called tie chains [3–6], have a determining role in elastic and plastic deformation of semicrystalline polymers. However, due to the molecular length scales involved, experimental studies are not able to discern the tie chains and resolve their contribution to the mechanical response. Here, we elucidate their essential role by examining the local deformation of chains in large-scale molecular dynamics (MD) simulations.

Semicrystalline samples are prepared by cooling a melt of a crystallizable polymer, described by linear bead-spring chains with an anharmonic bending potential [7]. This model was previously derived through coarse-graining of polyvinyl alcohol (PVA) [8]. Long polymers of the CG-PVA model form semicrystalline configurations that consist of randomly oriented crystallites with 2D hexagonal order connected by an amorphous entangled network as demonstrated in Fig. 1. This structure differs from prior work on the role of entanglements and tie chains in various deformation modes [9–11], which focused on a layered semicrystalline morphology as part of a larger spherulite structure.

We investigate the tensile response of amorphous and semicrystalline polymers with lengths $50 \leq N \leq 1000$ beads. This range spans lengths comparable to the entanglement length ($N_e = 32 \pm 2$ in the melt [12] and $N_e \approx 40$ in semicrystalline polymers [13]) to long chains with $N \gg N_e$. Characterization of the crystalline domains allows us to directly identify tie chains as the chain segments connecting them. We then investigate the influence of tie chains and crystallinity on the tensile response.

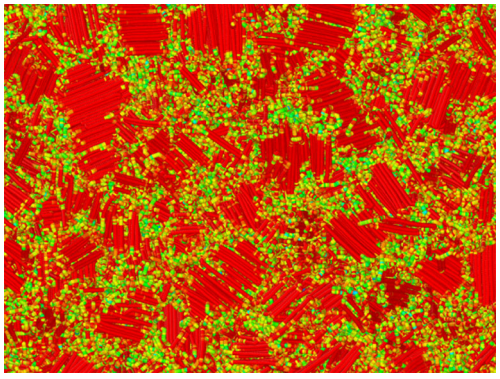

FIG. 1. An example of CG-PVA semicrystalline configurations with $N = 1000$ monomers that consists of chain-folded crystallites (red) connected by an amorphous network.

MD simulations are carried out using LAMMPS [14]. Distances are reported in units of $\sigma = 0.52$ nm, and the bond length is $b_0 = 0.5\sigma$. The range and strength of a 6-9 Lennard-Jones potential for nonbonded interactions are $\sigma_{LJ} = 0.89\sigma$ and $\epsilon = 1.511 k_B T_0$, where $T_0 = 550$ K is the reference temperature [7]. The Lennard-Jones potential is truncated and shifted at $r_c = 1.6\sigma$. Temperatures $T = T_{\text{real}}/T_0$ and pressures $P = P_{\text{real}}\sigma^3/\epsilon$ are reported in reduced units. We apply periodic boundary conditions and use a time step of 0.005τ. The melt configurations are prepared by equilibrating in the NPT ensemble ($T = 1.0$ and $P = 8$) [7] starting from an initial configuration of self-avoiding random walks with initial monomer density $\rho\sigma^3 = 2.11$. Our equilibration time is long enough to achieve full equilibration for chains with $N \leq 300$. Longer chains can only relax the chain segments between entanglements (Rouse time) although their mean-squared internal distances are not far from those of equilibrated chains. Nevertheless, we do not expect that our conclusions regarding the role of tie chains are strongly affected.

Larger melt samples of up to 2×10^6 monomers are then prepared by replicating the equilibrated melt configurations. We obtain semicrystalline and amorphous states by continuous cooling with constant rates of $\dot{T} = -10^{-6}\tau^{-1}$ and $\dot{T} = -10^{-3}\tau^{-1}$, respectively [15]. For $\dot{T} = -10^{-6}\tau^{-1}$, chains undergo a crystallization transition at $T_c \approx 0.9$ and transform into chain-folded structures immersed in a network of amorphous strands [7]. For the rapid quench, $\dot{T} = -10^{-3}\tau^{-1}$, polymers retain their amorphous configurations and undergo a glass transition. The glass transition temperature of fully amorphous samples T_g is determined from the change in slope of the specific volume versus T and is roughly constant, $T_g \approx 0.56$ for $N \geq 50$. In the following, T_g refers to the glass transition of purely amorphous systems.

Next, we investigate the chain length dependence of the mechanical response. We perform tensile tests by deforming the samples in the y direction with a constant true strain rate of $\dot{\epsilon} = 10^{-5}\tau^{-1}$ while imposing a constant pressure of $P = 8$ (as in undeformed samples) in the x and z directions [16]. The strain rate lies in the range $\tau_R^{-1} < \dot{\epsilon} < \tau_e^{-1}$ and, hence, holds each chain in a tubelike regime. Tensile tests of glassy and semicrystalline polymers with $N = 300$ for strain rates $10^{-7} < \dot{\epsilon} < 10^{-4}$ exhibit a very weak dependence on the strain rate. The volume increase is at most 3(6)% for the amorphous (semicrystalline) polymers at large strains and $T = 0.2$. Therefore, these systems behave nearly as an incompressible fluid.

Figures 2(a) and 2(b) present stress-strain curves for amorphous and semicrystalline polymers obtained at $T = 0.7 > T_g$ and $T = 0.2 < T_g$, respectively. For all samples, the elastic regime at small strains is followed by plastic flow at larger deformations. The plastic regime in semicrystalline polymers includes a strain plateau or softening

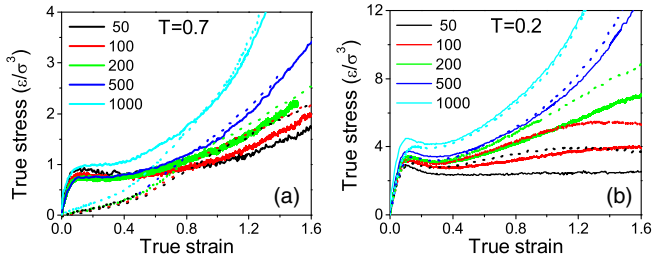

FIG. 2. Stress versus strain from uniaxial tensile deformation of semicrystalline (solid lines) and amorphous (dotted lines) polymers of different lengths at (a) $T = 0.7$ and (b) $T = 0.2$.

behavior beyond the yield point and strain hardening at larger deformations. At $T = 0.7 > T_g$, amorphous polymers are rubbery and their response consists of a large elastic region followed by strain hardening. Glassy polymers at $T = 0.2 < T_g$ exhibit a strain-softening regime followed by hardening at larger deformations. The amorphous polymers exhibit a stronger strain-hardening behavior than their semicrystalline counterparts.

To investigate the microscopic rearrangement of chains under macroscopic stretching, we measure the rms components R_i of the end-to-end vectors of chains relative to their initial values R_{0i} [17]. For a tensile deformation in the y direction, the changes in R_i are consistent with a volume-conserving effective microscopic stretch λ_{eff}, obtained as $\lambda_{\text{eff}} \equiv R_y/R_y^0 = (R_x^0/R_x)^2 = (R_z^0/R_z)^2$. An affine deformation corresponds to $\lambda_{\text{eff}} = \lambda \equiv L_y/L_y^0$. λ_{eff} was found to be the crucial parameter controlling the strain-hardening behavior of glassy polymers [17].

In Figs. 3(a) and 3(b), we display λ_{eff} as a function of the macroscopic stretch λ for semicrystalline and amorphous polymers of different N at $T = 0.7$ and $T = 0.2$, respectively. The deformation of short chains is smaller than the macroscopic stretch and they deform subaffinely. In particular, the semicrystalline polymers exhibit a larger degree of subaffine behavior. Semicrystalline polymers behave slightly less affine compared to their amorphous counterparts because chains within the crystallites deform less than purely amorphous chains. Upon increase of N, λ_{eff} increases and the difference between amorphous and

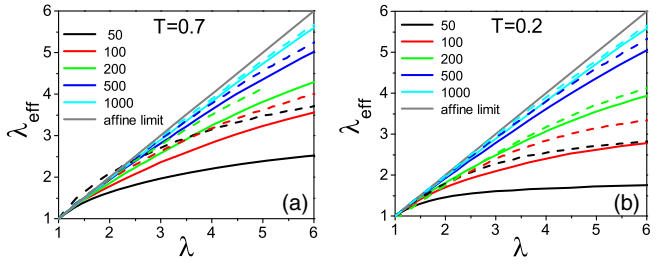

FIG. 3. Effective microscopic stretch $\lambda_{\text{eff}} \equiv R_y/R_y^0$ versus macroscopic stretch $\lambda \equiv L_y/L_y^0$ for semicrystalline (solid lines) and amorphous (dashed lines) polymers at (a) $T = 0.7$ and (b) $T = 0.2$.

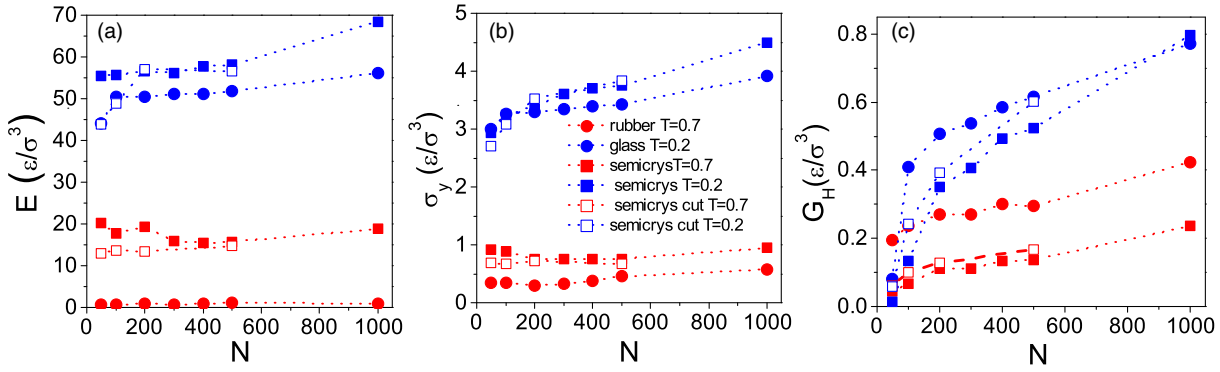

FIG. 4. Chain length dependence of (a) Young's modulus E, (b) yield stress σ_y, and (c) strain-hardening modulus G_H for amorphous and semicrystalline polymers obtained by continuous cooling and by cutting the chains of semicrystalline samples into half. For cut chains, N refers to their length after cutting (see text).

semicrystalline polymers becomes negligible. Notably, highly entangled systems approach the affine limit and their stress-strain curves also coincide.

To quantify the effect of N on the tensile response, we extract Young's modulus E, yield stress σ_y, and strain-hardening modulus G_H from stress-strain curves. E is determined from the slope of σ for $\epsilon < 0.05$. G_H is determined from the slope of σ versus $\lambda^2 - 1/\lambda$ at the initial stage of strain hardening, i.e., $0.4 < \epsilon < 0.9$. For glassy and semicrystalline polymers, σ_y is the maximum value of the stress in the overshoot region. For the rubbery polymers, σ_y is the crossover point between the elastic and the strain-hardening regimes. As demonstrated in Figs. 4(a)–4(c), the N dependence of E, σ_y, and G_H are remarkably different for temperatures above and below T_g.

At $T = 0.7 > T_g$, E and σ_y exhibit an irregular behavior against N. For $N > 200$, we find a constant $\sigma_y/E \approx 0.05$. In contrast to E, G_H increases systematically with N. At this temperature, Young's modulus of rubbery polymers is much smaller than in semicrystalline polymers and is independent of N. G_H of rubbery polymers grows with N and is even larger than for semicrystalline polymers. An increasing G_H with N is in disagreement with predictions of ideal rubber theories, in which chain segments between two consequent entanglements are assumed to deform affinely [18]. This trend is due to viscous contributions in supercooled melts as we approach T_g.

At $T = 0.2 < T_g$, we observe an enormous increase in the tensile response for glassy and semicrystalline polymers. For both systems, E and σ_y increase with N. Notably, glassy polymers also develop a substantial amount of elasticity and the difference between their elastic moduli and those of semicrystalline polymers is less pronounced. At this temperature, the intercrystalline amorphous network contributes significantly to the elasticity. We observe a constant $\sigma_y/E \approx 0.06$ for both semicrystalline and glassy polymers. Likewise, their G_H is an increasing function of N and its value is larger than G_H above T_g due to reduced chain mobility.

To understand the link between the tensile response and the underlying structure, we characterize the crystalline and amorphous regions. We identify crystalline domains by computing a local nematic order parameter in cubic boxes of size $\sim 2\sigma$, and performing a cluster analysis as detailed in Ref. [12]. The degree of crystallinity Φ_c is defined as the volume fraction of crystalline cells with a nematic order parameter $S > 0.8$. Bonds are labeled as ordered if they belong to a crystalline domain. We determine the average length of crystalline sequences L_c (stem length) from the size distribution of ordered segments along the chains.

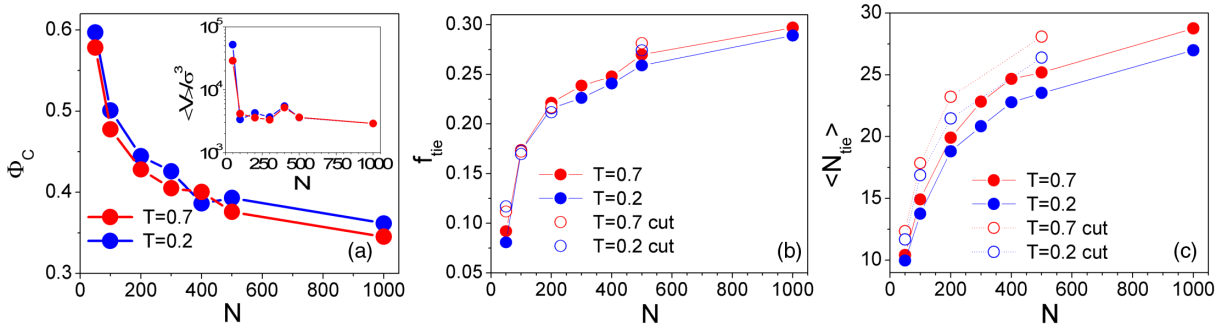

FIG. 5. (a) Degree of crystallinity Φ_c at $T = 0.2$ and $T = 0.7$ as a function of polymer length N; the inset shows the average volume of the crystalline domains. (b) Fraction of tie bonds f_{tie} and (c) the average length of tie strands $\langle N_{\text{tie}} \rangle$ versus N.

Figure 5(a) shows that Φ_c is a decreasing function of N as already observed for $N \leq 200$ [19]. The average length of crystalline sequences is almost constant, i.e., $L_c \approx 10$ independent of N and T. As demonstrated in the inset of Fig. 5(a), the average volume of crystalline domains decreases up to $N = 100$ and then levels off. These trends imply that increasing the number of entanglements per chain does not change the local structure of crystallites. Entanglements lead to a decrease of crystallinity by hindering the large-scale ordering of polymers, as the chains need to disentangle before they can form ordered structures [20].

The irregular behavior of E with N is in contrast to the systematic increase of E with Φ_c found for semicrystalline polymers of $N = 300$ [15]. Furthermore, at $T = 0.2$, we observe a remarkable increase of E and σ_y despite a declining Φ_c. Therefore, the hypothesis of an elastic modulus that depends directly on Φ_c, or a two-phase Kelvin-Voigt picture for E, are invalidated by those findings. Consequently, we investigate the effect of tie chains in the response as suggested by experiments.

We identify the tie chains as the intercrystalline amorphous strands with at least two bonds that connect two distinct crystalline domains. We define f_{tie} as the fraction of bonds belonging to tie chains relative to the total number of bonds. Figure 5(b) shows that f_{tie} rises with N, concomitant with a decrease of crystallinity, but it always remains smaller than the total fraction of amorphous chains, i.e., $1 - \Phi_c$. From the length distribution of tie chains, we obtain their average length $\langle N_{\text{tie}} \rangle$, i.e., the number of bonds in a strand. Figure 5(c) shows that $\langle N_{\text{tie}} \rangle$ also increases with N while the number density of tie strands shows a small variation; for $50 < N \leq 1000$ we find that ρ_{tie} decreases from $0.029\sigma^{-3}$ to $0.026\sigma^{-3}$. The increase of f_{tie} directly leads to an increase in $\langle N_{\text{tie}} \rangle$ and could possibly rationalize the N dependence of E and G_H.

To assess the contribution of tie chains to the tensile response, we cut the chains of semicrystalline samples with length $N = 100, 200, 400$, and 1000 into half. This process generates new semicrystalline samples with chain length $N/2$ that have a lower crystallinity than samples with the same chain length obtained by continuous cooling and with almost identical f_{tie} for $N > 50$, as shown in Fig. 5(b). However, their tie chains are on average slightly longer due to decrease of crystallinity as presented in Fig. 5(c). We measure the tensile response of the semicrystalline samples generated by this protocol and compare to uncut polymers of length N and $N/2$.

Figures 6(a) and 6(b) present the tensile response of cut and uncut chains at $T = 0.7$ and $T = 0.2$, respectively. Half-cut chains with length $N/2$ exhibit a very similar mechanical response to uncut chains of length $N/2$. On the other hand, semicrystalline polymers of length N with identical ϕ_c and larger f_{tie} present a different mechanical response, highlighting the importance of tie chains and

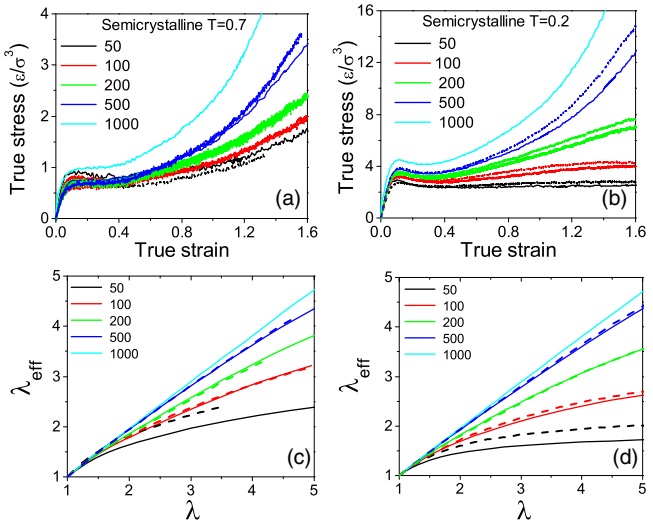

FIG. 6. (a),(b) Stress versus strain and (c),(d) effective microscopic stretch versus macroscopic stretch for semicrystalline polymers of various lengths obtained from continuous cooling (solid lines) and from cutting of polymers into half (dashed lines) at $T = 0.7$ and $T = 0.2$, respectively.

chain length. The extracted moduli of cut chains are included in Fig. 4. We observe a general trend that decreasing f_{tie} and N but keeping Φ_c constant reduces E, σ_y, and G_H to lower values close to those of shorter uncut chains with almost identical f_{tie}. Comparing average end-to-end distance of tie chains to purely amorphous polymers with the same length, we find that tie chains are prestretched during crystallization. Hence, they affect the mechanical behavior even in the elastic regime.

Next, we compare the effective stretch of cut chains to λ_{eff} of uncut samples, as shown in Figs. 6(c) and 6(d). We find that λ_{eff} of cut chains is the same as those of uncut chains with the same length, when their f_{tie} is almost identical, i.e., for the case $N > 50$. In the case of $N = 50$, where the cut chains have a higher f_{tie} than the uncut ones, we observe a larger degree of microscopic stretch for the cut chains; again emphasizing the role of tie chains in microscopic chain rearrangements. The tensile response of semicrystalline polymers is controlled by the overall global stretch that itself depends on f_{tie} and number density of entanglements. Our local chain-deformation analysis provides a new microscopic insight into underlying mechanisms of plastic deformation in semicrystalline polymers. Our results expand on previous findings for purely glassy polymers [17] in which the effective microscopic stretch controls the strain-hardening behavior.

We conclude by summarizing our main findings. The tensile response of semicrystalline polymers is a strong function of chain length and is remarkably different for temperatures above and below T_g. Long polymers form chain-folded crystalline structures that are interlocked by amorphous networks of entanglements and tie chains. The

loss of a fraction of the entanglement network [20] upon crystallization is partially compensated by tie chains that contribute to the response. Analysis of the microscopic stretch of chains under tensile deformation suggests that the response of heterogeneous semicrystalline polymers follows from superposition of interpenetrated networks of tie chains and entanglements in agreement with experiments [3–6]. Longer polymers give longer tie segments, with lengths comparable to the entanglement length, that enforce affine deformation at all scales in a manner similar to entanglements in purely amorphous systems. Nevertheless, the tie chains are on the average shorter than the entanglement length and therefore are not themselves entangled.

The semicrystalline morphologies of randomly orientated crystallites obtained in our simulations are far from the experimental spherulitic ones. Still, they mimic most of the classical mechanical behavior of semicrystalline polymers. Our study shows that general structural features of semicrystalline polymers, i.e., chain topology (tie chains and entanglements) and crystallinity, govern their general mechanical response. Predicting the functional dependence of the moduli on structural parameters Φ_c, f_{tie}, and N/N_e, however, remains a challenge for theories of polymer deformation. Furthermore, the insights from this study could be relevant for composite polymeric materials with ordered regions connected by linkers [21] or biopolymer networks consisting of regions of ordered beta sheets embedded in an amorphous network [22,23].

Computations were performed using the Froggy platform of the CIMENT infrastructure supported by the Rhône-Alpes region (Grant No. CPER07-13 CIRA) and the Equip@Meso Project (Reference 337 No. ANR-10-EQPX-29-01). S. J.-F. acknowledges financial support from the German Science Foundation within SFB TRR 146. J.-L. B. is supported by Institut Universitaire de France and by Grant No. ERC-2011-ADG20110209.

*Corresponding author.
sjabbari@uni-mainz.de

[1] G. H. Michler and F. J. Balta-Calleja, *Mechanical Properties of Polymers Based on Nanostructure and Morphology* (Taylor & Francis group, New York, 2005).
[2] E. F. Oleinik, S. N. Rudnev, and O. B. Salamatina, Polym. Sci., Ser. A **49**, 1302 (2007).
[3] Y. Men, J. Rieger, and G. Strobl, Phys. Rev. Lett. **91**, 095502 (2003).
[4] S. Humbert, O. Lame, and G. Vigier, Polymer **50**, 3755 (2009).
[5] S. Humbert, O. Lame, R. Séguéla, and G. Vigier, Polymer **52**, 4899 (2011).
[6] R. Seguela, J. Polym. Sci., Part B: Polym. Phys. **43**, 1729 (2005).
[7] H. Meyer and F. Muller-Plathe, J. Chem. Phys. **115**, 7807 (2001).
[8] H. Meyer and F. Muller-Plathe, Macromolecules **35**, 1241 (2002).
[9] S. Lee and G. C. Rutledge, Macromolecules **44**, 3096 (2011).
[10] J. M. Kim, R. Locker, and G. C. Rutledge, Macromolecules **47**, 2515 (2014).
[11] I.-C. Yeh, J. W. Andzelm, and G. C. Rutledge, Macromolecules **48**, 4228 (2015).
[12] S. Jabbari-Farouji, J. Rottler, O. Lame, A. Makke, M. Perez, and J. L. Barrat, J. Phys. Condens. Matter **27**, 194131 (2015).
[13] C. Luo and J.-U. Sommer, Phys. Rev. Lett. **112**, 195702 (2014).
[14] S. Plimpton, J. Comput. Phys. **117**, 1 (1995).
[15] S. Jabbari-Farouji, J. Rottler, O. Lame, A. Makke, M. Perez, and J. L. Barrat, ACS Macro Lett. **4**, 147 (2015).
[16] See Supplemental Material at http://link.aps.org/supplemental/10.1103/PhysRevLett.118.217802 for a visual inspection of conformational changes of semicrystalline polymers during tensile deformation.
[17] R. S. Hoy and M. O. Robbins, Phys. Rev. Lett. **99**, 117801 (2007).
[18] L. R. G. Treloar, *The Physics of Rubber Elasticity* (Clarendon Press, Oxford, 1975).
[19] V. Triandafilidi, J. Rottler, and S. G. Hatzikiriakos, J. Polym. Sci., Part B: Polym. Phys. **54**, 2318 (2016).
[20] C. Luo and J. Sommer, ACS Macro Lett. **2**, 31 (2013).
[21] H. Cho, J. C. Weaver, E. Poeselt, P. J. in't Veld, M. C. Boyce, and G. C. Rutledge, Adv. Funct. Mater. **26**, 6938 (2016).
[22] M. A. Brenckle, B. Partlow, H. Tao, D. L. Kaplan, and F. G. Omenetto, Biomacromolecules **14**, 2189 (2013).
[23] Y. Yoshimura, Y. Lin, H. Yagi, Y.-H. Lee, H. Kitayama, K. Sakurai, M. So, H. Ogi, H. Naiki, and Y. Goto, Proc. Natl. Acad. Sci. U.S.A. **109**, 14446 (2012).